J Genet Resour 2023; 9(2): 232-243 *Homepage: http://sc.journals.umz.ac.ir/*

RESEARCH ARTICLE *DOI: 10.22080/jgr.2023.25719.1367*

Controlled Release of Curcumin by Graphene Oxide/Chitosan/Sodium Alginate Hydrogel Multilayer Nanocomposites and Evaluate its Synergistic Antibacterial Activity

Shirin Soltani and Arastoo Badoei-Dalfard*

Department of Biology, Faculty of Sciences, Shahid Bahonar University of Kerman, Kerman, Iran

ARTICLE INFO

Article history:
Received 05 May 2023
Accepted 09 July 2023
Available online 23 July 2023

Keywords:
Antibacterial activity
Curcumin
Drug loading
Hydrogel multilayer

****Corresponding authors:***
✉ A. Badoei-Dalfard
badoei@uk.ac.ir

p-ISSN 2423-4257
e-ISSN 2588-2589

ABSTRACT

Curcumin has many medical properties, such as anti-inflammatory, anti-microbial, antioxidant, and anti-tumor activities. However, its hydrophobic nature results in less solubility and fast metabolism. Nowadays, designing a cargo based on nano-biotechnology is an efficient method to overcome these limitations of curcumin. This study synthesized graphene oxide/chitosan/sodium alginate (GCA) multilayer nanocomposites according to a layer-by-layer (LBL) assembly to load curcumin. Firstly, for graphene oxide/chitosan (GC) nanocomposite synthesis, graphene oxide (G) suspension was added to the chitosan (CS) solution dropwise during stirring. Then, sodium alginate (A) in water was added to the GC suspension drop wisely, centrifuged, and lyophilized. This GCA multilayer nanocomposite showed a layered structure with negative zeta potential. Though the drug loading efficiency of this GCA multilayer was not as high as graphene oxide, its curcumin release was pH-dependent. The highest drug release belonged to GCA due to the presence of curcumin in the hydrogel network without tight binding. This release was pH-dependent as the curcumin release after 24 h was 80% in pH 5 for GCA, while this amount was 60 % in pH 7 because of hydrogel network disruption in the acidic environment. The antibacterial results exhibited that this GCA multilayer did not show any antibacterial activity. It was significant that curcumin did not affect *E. coli*, though the minimum inhibitory concentration (MIC) for *S. aureus* was 300 µg/ml. Ciprofloxacin has been used to investigate the effect of GCA nanocomposite's synergetic release of curcumin and antibiotics. Results showed that ciprofloxacin increased the inhibition zone diameter for *S. aureus*, but this was not observed in *E. coli*. Overall, it can be concluded that the antibacterial activity of curcumin is not evitable. To explain this, the antioxidant activity of curcumin, which reduces the radicals due to ciprofloxacin activity, can be considered.

© 2023 University of Mazandaran

Please cite this paper as: Soltani, S., & Badoei-Dalfard, A. (2023). Controlled release of curcumin by graphene oxide/chitosan/sodium alginate hydrogel multilayer nanocomposites and evaluate its synergistic antibacterial activity. *Journal of Genetic Resources*, *9*(2), 232-243. doi: 10.22080/jgr.2023.25719.1367

Introduction

Turmeric, an eastern condiment, is obtained from Curcuma longa rhizomes and used in traditional medicine to treat infections, inflammations, *etc*. The major compound of turmeric is curcumin, which is responsible for turmeric's yellow color. Today, curcumin's biological activity has been taken into consideration. Many studies have revealed its antioxidant, antibacterial (Moghaddam *et al*., 2009: Mehrabi *et al*., 2021: Mehrabi *et al*., 2022), antifungal, anti-apoptotic, anti-proliferative, and anticancer activity (Lim *et al*.,

This work is licensed under the *Creative Commons Attribution 4.0 International License.*

2001; Hussain *et al*., 2017; Zheng *et al*., 2020). Despite these significant characteristics, curcumin bioavailability and stability are very low, which limits its usage. As mentioned above, its solubility is very low in the water, so it has poor dispersion in biological solutions (Chidambaram and Krishnasamy, 2014; Mehrabi *et al*., 2022). Curcumin has a fast metabolism in the body (by sulfonation, conjugation, and glucuronidation). On the other hand, enzymes degenerate curcumin into an unusual compound, and some pumps exclude this compound (Jamil *et al*., 2017). Therefore, only <1% of curcumin enters the bloodstream. However, curcumin can easily pass through the biological membrane because of its lipophilic nature (Helson, 2013).

Diverse methods were employed to overcome the limitations of curcumin (Li *et al*., 2020). In recent decades, nanotechnology has attracted much attention to eliminating these limitations and evaluating drug delivery. Nanosystems like polymeric nanoparticles, liposomes, nanohybrid scaffolds, hydrogel nanocomposites, nanofibers, and nanofilms have been designed for curcumin delivery (Ma *et al*., 2008). These systems protect the cargo from enzymatic degeneration, create a controlled release, enhance solubility pharmacokinetic characteristics, target drug delivery, and increase the shelf time of the drug in plasma. Graphene oxide is a nanostructure that contains one layer of carbon atoms as a honeycomb network. It is the thinnest and strongest compound in the world (Zhu *et al*., 2010). Because of their high surface area, nano size, and facilitated functionalization, graphene oxide (G) based structures have recently been chosen as candidates for drug delivery. Therefore, graphene is used as cargo for several drugs, especially less soluble anticancer and antimicrobial drugs (Pan *et al*., 2012). Based on these studies, curcumin can bind to graphene nanosheets by π-π interaction (Ramazani *et al*., 2018). However, toxicity and biocompatibility are the main concerns for graphene and its derivatives applications because of the acidic nature of graphene and the toxic chemicals for its production (Zhang *et al*., 2011; Wong *et al*., 2017). Also, aggregation in salted media is another limitation. Therefore, bioavailability is crucial to modifying the graphene surface to evaluate its biocompatibility (Wong *et al*., 2017). Changing the graphene surface by hydrogel is very noticeable. Hydrogels are very hydrophobic networks that can store a high amount of water, have excellent permeability for small molecules, and are like the body's tissues. Moreover, they can cover the sharp edges of the graphene nanosheets (Ghawanmeh *et al*., 2019; Nurunnabi *et al*., 2015). There are several nanotechnology methods for graphene modifications by hydrogels. Among these methods, LBL self-assembly is an effective method due to the ease of work, cost-effectiveness, and variety of materials used (Hu and Mi, 2014). This method is based on encountering a substrate with polyelectrolyte solutions. Because of the dependence of this method on polyelectrolyte charge and concentration, LBL structures can be controlled easily (Richardson *et al*., 2016).

Chitosan is biocompatible and biodegradable, and its surface positive charge is feasible for layer-by-layer deposition. Sodium alginate (A) could act as a shield to diminish the rush release of the drug due to suitable viscosity. It could also form a three-dimensional network structure in a physiological environment and reduce the negative charge on the surface (Wang *et al*., 2018).

This study produced graphene oxide/chitosan/sodium alginate (GCA) multilayer nanocomposites to load curcumin. According to the LBL method, these nanocomposites were produced by depositing chitosan and sodium alginate hydrogels on graphene. Then, its physicochemical and biological activity was investigated. The loading efficiency and drug release were measured, and these compounds were finally tested for antibacterial activity.

Materials and Methods

Chitosan, sodium alginate, bovine serum albumin (BSA), ciprofloxacin, graphite flakes, and curcumin were purchased from Merck (Germany). Muller Hinton broth and agar were obtained from Scharlau (Spain).

Graphene oxide synthesis

In this study, Graphene Oxide (GO) was prepared using the modified Hummer method (Zaaba *et al*., 2017). Briefly, graphite powder was pretreated by mixing with H_2SO_4 and HNO_3

with a 3:1 ratio. After 24 hours, 120 ml of deionized water was added to quench the reaction. This mixture was centrifuged and rinsed with deionized water, and the precipitant was lyophilized. In the next step, the product was treated with H_2SO_4, and by putting the bottle in an ice bath, 300 mg $KMnO_4$ powder was gradually added, and the color of the solution became green. After 24 hours, by adding deionized water, the temperature of the reaction decreased to 25 °C. The aquatic solution of H_2O_2 with a 3:1 ratio was added at this time. The final product was centrifuged at 4000 rpm for 10 min. At last, the precipitant was washed with HCl (37%) and deionized water, respectively. The brownish precipitant was lyophilized (Telstar Freeze-dryer).

Graphene oxide/chitosan synthesis

Graphene powder was dispersed in 60 ml of deionized water by water bath sonication until a clear brownish suspension was obtained. Chitosan solution with 0.2 mg/ml concentration in acid acetic (0.6% v/v) was prepared. The pH of the solution was adjusted to 5.5-6.5 by NaOH, and the volume increased to 60 ml (Zokaei *et al*., 2019; Badoei-Dalfard *et al.*, 2022). For Graphene oxide/Chitosan (GC) nanocomposite synthesis by the LBL method (Wang *et al*., 2018), GO suspension was added to the CS solution dropwise during stirring. The mixture was centrifuged at 4500 rpm for 30 min, washed with deionized water, and lyophilized.

Graphene oxide/chitosan/sodium alginate synthesis

For GC nanocomposite synthesis, by the LbL method, graphene suspension was added to the CS solution dropwise during stirring. Sodium alginate (A) solution (0.2 mg/ml) in water was wisely added to the GC suspension drop, centrifuged like the previous step, and lyophilized to obtain the graphene oxide/chitosan/sodium alginate.

Physicochemical characterization

The Fourier Infrared Spectrum (FTIR) was analyzed by TENSOR 27. The zeta potential of each nanocomposite was calculated using a ZEN3600 zeta sizer. The morphology of nanocomposites was investigated by Transmission Electron Microscopy (TEM) (LEO912-AB). Dynamic Light Scattering (DLS) was done by Horiba SZ100 to analyze the size. The absorption was calculated by Biowave WPA.

BSA absorption

Non-specific protein absorption was investigated by BSA absorption. So, BSA solution in PBS (1mg/ml, pH 7.4) was added directly to each nanocomposite suspension during stirring. After 24 h, the supernatant was gathered by centrifuging the mixtures, and their absorbance was measured at 280 nm.

Hemolysis

Fresh blood from Afzalipour Hospital (Kerman, Iran) was obtained and kept in sodium heparin tubes to block coagulation. The serum of each sample was removed by centrifugation. 0.2 ml of diluted blood with PBS was mixed with 0.8 ml of nanocomposite suspension and incubated at 37 °C for 3 h. Blood samples diluted with PBS and water were chosen as positive and negative controls, respectively. The supernatant absorptions were read at 540 nm.

Hemolysis (%) = (A-pAn-Ap)×100, in which A is sample absorption, Ap is positive control absorption, and An is negative control absorption.

Drug loading

20 ml of ethanolic solution of curcumin (0.5 mg/ml) was added to each nanocomposite suspension (0.2 mg/ml). After 24 h, the mixtures were centrifuged at 4500 rpm and rinsed with distilled water. The supernatant absorption was read at 420 nm.

Drug loading efficiency = $(W_1\text{-}W_2/W_1)\times100$, in which W_1 is the weight of the total drug, and W_2 is the weight of the free drug.

Drug release

Drug release was measured by the dialysis method. According to this method, suspensions of nanocomposites loaded with curcumin were prepared in PBS and transferred to dialysis bags (10 kDa cut-off). These bags were immersed in PBS with two different pH 7 and 5.4 containing 12, 20 (0.2% v/v) and were placed in a shaker incubator at 37 °C. In various time intervals, an

amount of liquid around the bags was picked up, and an equal amount of fresh PBS was replaced (Jalaladdiny *et al.*, 2022). The amount of released curcumin was measured by a fluorescent spectrophotometer (Biotek) (absorbance in 480 nm and transmittance in 550 nm).

Antibacterial activity

For antibacterial activity, *S. aureus* and *E. coli* were obtained from the microbiology lab faculty of veterinary medicine (Kerman). The new culture was prepared in MHB and incubated for 24 hours at 37 °C. Disk diffusion and serial dilution methods were selected for antibacterial activity investigation. Curcumin solution: curcumin stock with 10 mg/ml was prepared in ethanol and then combined with MHB to obtain a clear solution with 1 mg/ml concentration. This solution was used to prepare serial dilutions (0.01 to 0.06 mg/ml). Nanocomposite suspension: nanocomposite with or without curcumin (1mg/ml) was dispersed in phosphate-buffered saline (PBS) by sonication.

Investigation of the synergistic effects

Disc diffusion of different nanocomposites (1; G, 2; GC, and 3; GCA) carrying curcumin in the presence and absence of ciprofloxacin (Cip) has been done on the *E. coli* and *S. aureus* plates. Different samples have been used, such as 1) curcumin (300 µg), 2) curcumin (300 µg) with ciprofloxacin, 3) curcumin (200 µg) with ciprofloxacin, 4) curcumin 100 µg with ciprofloxacin, 5) ciprofloxacin in solvent (DMSO), 6) Ciprofloxacin in water, and 7) solvent (DMSO). Ciprofloxacin concentration was 50 µg/disk in all experiments.

Results and Discussion

Graphene oxide synthesis

Graphene oxide is obtained in different ways. In the Hummer method, graphene oxide can be prepared from the oxidative exfoliation of graphite by H_2SO_4, HNO_3, and $KMnO_4$ (Zokaei *et al*., 2019). The conversion of the color of graphite powder from black to brown shows graphene has been made, and a peak in 260 nm in the UV-vis spectrum of graphene confirms its synthesis (Fig. 1A). Moreover, the FTIR spectrum shows the presence of active oxygen groups on graphene nanosheets (Fig. 1B).

FTIR

An increase or decrease in the intension of peaks in the FTIR spectrum of nanocomposites (compared with G, CS, and A alone) demonstrates the addition of layers. By CS deposition on G nanosheets, a peak in 1580 cm^{-1} appeared, which shows the presence of NH_2 groups. Also, peaks in 1405 cm^{-1} and 1069 cm^{-1} are related to C-H and C-O groups of CS, respectively. The FTIR spectrum of GCA shows other peaks. A peak in 1560 cm^{-1} belongs to carboxylate vibration, and 1427 cm^{-1} is for C-O-C tensional vibration. The intension of the peak in 3000 cm^{-1} was decreased, revealing the well-covered nanocomposite by SA (Fig. 1B).

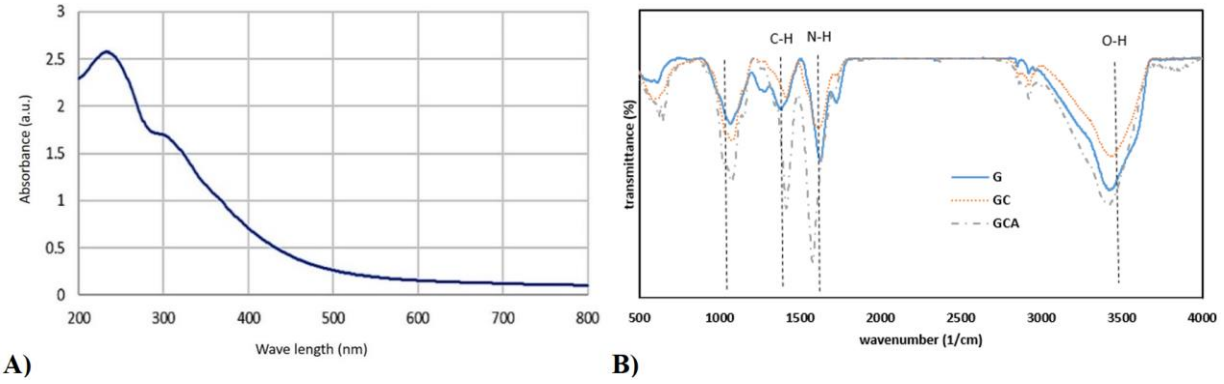

Fig. 1. Physicochemical characterization: A) UV-Vis spectrum of graphene oxide, B) FTIR spectrum of different nanocomposites.

DLS

Size and polydispersity of particles are essential parameters determining the nanoparticle dispersion, biological process, toxicity, and target capability. As Table 1 shows, polydispersity is high, and the reason for this is the two-dimensional nature of the graphene nanosheet. So, the new layer cannot deposit graphene equally in three dimensions. Also, shear forces that are the result of CS and alginate viscosity prevent particle formation with similar size (Wang *et al*., 2018). After the deposition of each layer, the size of nanocomposites has been increased. For GCA nanocomposites, this size increment is more considerable than for GC nanocomposites (3.88% versus 1.11%). As FTIR and TEM images of GCA show, a thick SA layer surrounds the nanocomposite, producing a thick hydrogel layer. Many studies show particles with a size below nanometer are better than microparticles for drug delivery systems (Desai *et al*., 1996). Typically, nanoparticles demonstrate higher cellular uptake than microparticles. Also, nanoparticles can penetrate the submucosal layer and cross the blood-brain barrier. While G and GC nanocomposites were below 1 micrometer, GCA reached 3 µm. Therefore, the route for its usage of this nanocomposite should be chosen carefully.

Table 1. DLS results of nanocomposites.

Graphenes	Poly Dispersity	Size (nm)
G	0.803	80.74
GC	0.989	91.77
GCA	1.0	314

Zeta potential

Zeta potential importance is related to nanoparticle interactions with each other and the environment. This parameter is affected by functional groups on the structure surface. High and the same zeta potential resulted in electrostatic repulsion, which prevents precipitation. Zeta potential may also determine how to deposit a new layer (surface absorption or penetration to structure) (Mu and Feng, 2003). So, ionic polymer deposition can be a significant step that changes the zeta potential of the structure. After adding each layer, the surface charge changed significantly. The zeta potential of graphene nanosheets alone was -25.9 mv due to hydroxyl and epoxy groups. But by adding CS, a polycationic polymer, zeta potential became positive (+23.42 mv). As expected, the presence of SA changed the surface charge to -26.93 mv due to carboxylic groups (Fig. 2). These results demonstrate that these layers were deposited based on LBL assembly because the zeta potential of the new layer became opposite to the previous layer.

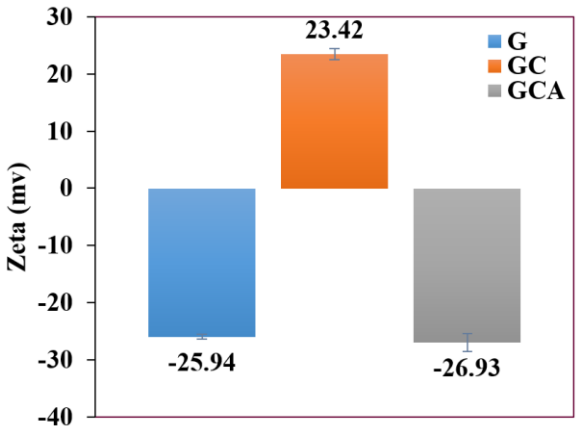

Fig. 2. Zeta potential of different nanocomposites: Graphene oxide (G), Graphene oxide/chitosan (GC), Graphene oxide/chitosan/sodium alginate (GCA).

TEM

As TEM images show, graphene nanosheets were surrounded by a thin layer of CS. By depositing the SA layer, the LBL structure of the particle is apparent (Fig. 3).

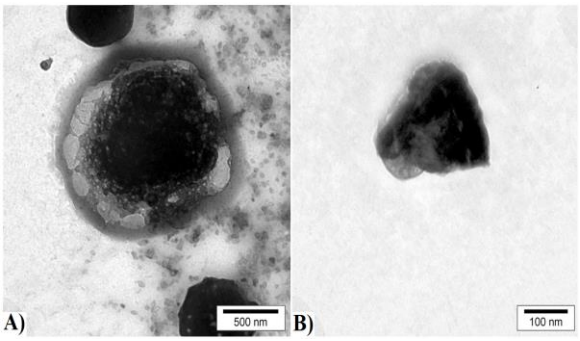

Fig. 3. TEM image of Graphenes: A) Images of Graphene oxide/chitosan/sodium alginate (GCA) NPs exhibited a core-shell morphology, in which sodium alginate shielded the Graphene oxide/chitosan (GC) nanoparticles; B) Images of GC.

Hemolysis

As the results show, the synthesized nanocomposites have different hemolytic

activity. Determinant factors of the hemolytic activity of nanoparticles are physical (sharp edges collision) and chemical interactions (electrostatic interactions) with red blood cells/RBCs (Kiew *et al*., 2016). As Fig. 4 shows, the highest hemolysis activity belonged to graphene. Based on TEM images, graphene nanosheets have sharp edges that cause membrane disruption and lysis. On the other hand, the surface of the RBCs has a negative charge due to glucose aminoglycan groups; therefore, ionic interactions that lead to lysis are considerable. So, between GC and GCA nanocomposites (positive and negative zeta potential, respectively), GC had higher hemolytic activity due to its absorption to RBCs surface by electrostatic interactions that resulted in membrane disruption (Fig. 4).

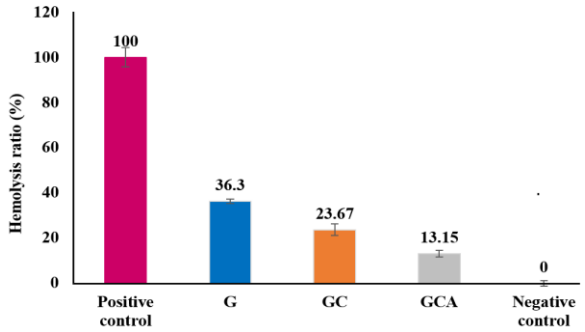

Fig. 4. Hemolysis activities of different nanocomposites: Graphene oxide (G), Graphene oxide/chitosan (GC), Graphene oxide/chitosan/ sodium alginate (GCA).

Nonspecific protein adsorption

By intravenous injection of nanoparticles, particles are detected by the immune system and cleaned by macrophages through opsonization, which is caused by blood protein adsorption. A particle's size, hydrophobicity, and surface charge affect protein absorption, which leads to opsonization (Yadav *et al*., 2012). In this research, graphene absorbed 50.34% of BSA due to the presence of hydrophobic groups. After modifying graphene by CS, BSA adsorption was increased to 69 % due to electrostatic interaction. However, the presence of the sodium alginate layer on the surface of the nanocomposite decreased the BSA absorption significantly due to high hydrophilicity and its negative surface charge (Fig. 5). Therefore, GCA nanocomposite can be a good candidate for safe consumption.

Drug loading

The UV-Vis spectrum of different curcumin concentrations was obtained, and its standard curve was drawn (Fig. 6). Drug loading depends on drug solubility in matrix or polymer, which is affected by polymer composition, polymer or matrix interaction, and the presence of the functional groups. In this study, the absorption method loaded the drug (curcumin). The most loading efficiency belongs to graphene (92%). Many studies proved graphene's high capacity in loading of different materials like drugs due to its high surface area and its various functional groups (Sun *et al*., 2008). Especially for curcumin loading, π-π bindings have a significant role because of the hydrophobic nature of curcumin.

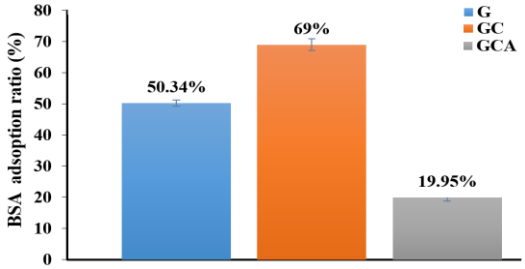

Fig. 5. BSA adsorption ratio of different nanocomposites: Graphene oxide (G), Graphene oxide/chitosan (GC), Graphene oxide/chitosan/ sodium alginate (GCA).

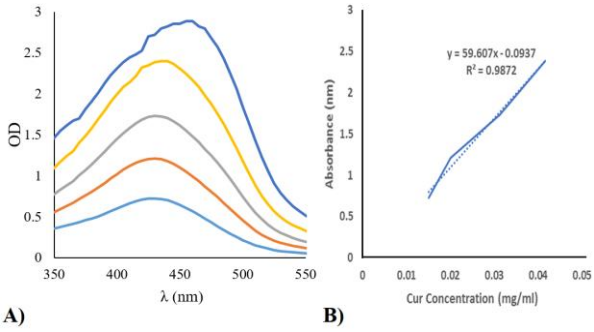

Fig. 6. UV-Vis spectrum and standard curve of curcumin: A) UV-Vis spectrum of different concentrations of curcumin; B) Standard curve of curcumin.

Loading curcumin on GC nanocomposite, although phenolic groups of curcumin tend to amino groups of CS, was very low (37.46% wt). The reason is related to the decrement of CS ionization, which fills amino group capacity (Yadav *et al*., 2012). Therefore, phenolic groups cannot bind to them, and loading is reduced. Curcumin loading efficiency in GCA nanocomposite was 59.30%, higher than GC loading efficiency. Though GCA has low amino groups and high hydrophilicity, the increment in curcumin loading is interesting. To explain this event, a complex network of CS and A can be considered, which traps curcumin in its structure, as illustrated in Figure 7 (Yadav *et al*., 2012).

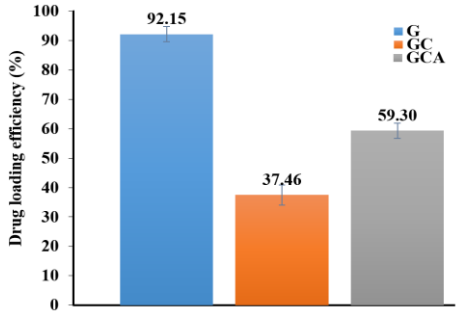

Fig. 7. Drug loading efficiencies of different nanocomposites: (Graphene oxide (G), Graphene oxide/chitosan (GC), Graphene oxide/chitosan/ sodium alginate (GCA)).

Drug release

For designing drug carriers, special attention has been paid to drug release in the acidic environment because infectious and tumor environments are acidic (Raja *et al*., 2017). Therefore, drug delivery can be targeted. Drug release depends on many parameters, including solubility, excretion of the adsorbed drug, drug diffusion through the matrix, and matrix disintegration, which can affect the release mechanism. The diffusion process controls the release mechanism whenever drug diffusion is faster than matrix decomposition. On the other hand, the weak binding of the drug to the matrix causes fast release (explosive release) (Bennis *et al*., 1994). Besides these, loading the drug is an important step, as loading after nanocomposite synthesis or during its synthesis leads to faster or slower release. The size of the particle is also crucial in that tiny particles have a large surface area, which can adsorb more drugs and lead to faster release (Panyam *et al*., 2004). In this study, all three nanocomposites showed rapid release in the first 24 h, resulting from curcumin loading after nanocomposite synthesis. The highest release belonged to GCA due to the presence of curcumin in the hydrogel network without tight binding. This release was pH-dependent as the curcumin release after 24 h was 80% in pH 5 for GCA, while this amount was 60 % in pH 7 because of hydrogel network disruption in the acidic environment (Fig. 8). Curcumin release from G in acidic and neutral pH was not different considerations due to π-π interaction. Though CS can be dissolved in an acidic environment, the high tendency of curcumin to amino groups of CS leads to low curcumin release in GC nanoparticles. Therefore, in this case, curcumin release did not significantly differ at various pH levels. From these results, it could be concluded that the chemical binding of curcumin with nanocomposite (in G and GC nanocomposites) prevents curcumin release because the hydrophobicity of curcumin decreases curcumin's tendency to disperse in a saline environment; therefore, physical binding could be better in this case.

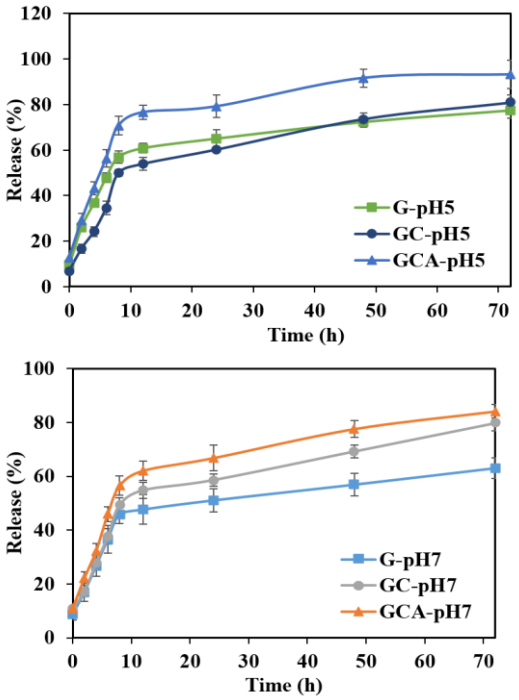

Fig. 8. Curcumin release of different nanocomposites in different pH (5.0 and 7.0).

Antibacterial effects

Antibacterial results showed that curcumin alone negatively affected on *S. aureus* growth (MIC= 300 µg/ml). Additionally, it did not have any considerable influence on *E. coli* (Table 2). The antibacterial effects of curcumin are limited to the bacteria species, just in a limited concentration range. Itzia Azucena *et al*. found curcumin alone had no impact on *E. coli* (Itzia-Itzia Azucena *et al*., 2019). However, unlike the results of the present studys, Gyu et al. realized curcumin causes an apoptotic response in *E. coli* (Yun and Lee, 2016). Also, Mun et al. confirmed the antibacterial effect of curcumin on *S. aureus* (Mun *et al*., 2013). These controversial results may result from using a different strain of bacteria or the different methods of curcumin stock preparation (Zheng *et al*., 2020). Investigation of the synergistic effects of curcumin with ciprofloxacin displayed significant results. Based on these results, the inhibition zone of *S. aureus* was 15 cm for curcumin. Similar to the previous results, using ciprofloxacin made this zone more significant than the obtained synergistic activity of these compounds (Mun *et al*., 2013; Roudashti *et al*., 2017; Teow and Ali, 2015). Meanwhile, the increase in curcumin concentration led to an increase in the inhibition zone of *S. aureus*. In the case of *E. coli*, these results were different. By curcumin concentration increment, the inhibition zone of *E. coli* became smaller. Significantly, the inhibition zone of the lowest curcumin concentration with ciprofloxacin was more significant than the ciprofloxacin alone (Fig. 9A). To explain the cause of these results, it could be said that the antioxidant activity of curcumin may be decisive. Based on other studies, antibiotics like ciprofloxacin lead to radical production in bacteria, which causes death (Goswami *et al*., 2006). Antioxidants like vitamin C and curcumin eliminate these radicals and protect bacteria. Masada et al. showed that the inhibition zone diameter decreased significantly using of vitamins C and D (Surdjawidjaja, 2012). Also, Moghaddam *et al*. proved the antagonistic impact of curcumin and nalidixic acid (Moghaddam *et al*., 2009). These results suggest that concomitant use of antibiotics would lead to synergism for species affected by curcumin's antibacterial activity. On the other hand, species not affected by curcumin's antibacterial activity were protected against antibiotics by the presence of curcumin and its antioxidant activity. None of the nanocomposites showed any antibacterial effects even when loaded with curcumin (Fig. 9B), which may be due to the slow release of curcumin in agar. Only in the case of GC-cur and GCA-curcumin was the inhibition zone created. Based on other studies, chitosan has antimicrobial effects, and this property helped curcumin show its antimicrobial effects in this study. Adding ciprofloxacin led to the appearance of zone inhibition for *S. aureus* (Table 3). The most significant inhibition zone was GCA, which related to the high curcumin release in GCA nanocomposite based on release results. However, for *E. coli*, the size of zone inhibition was equal for each nanocomposite, demonstrating that curcumin does not have any synergistic effect with ciprofloxacin (Fig. 9C).

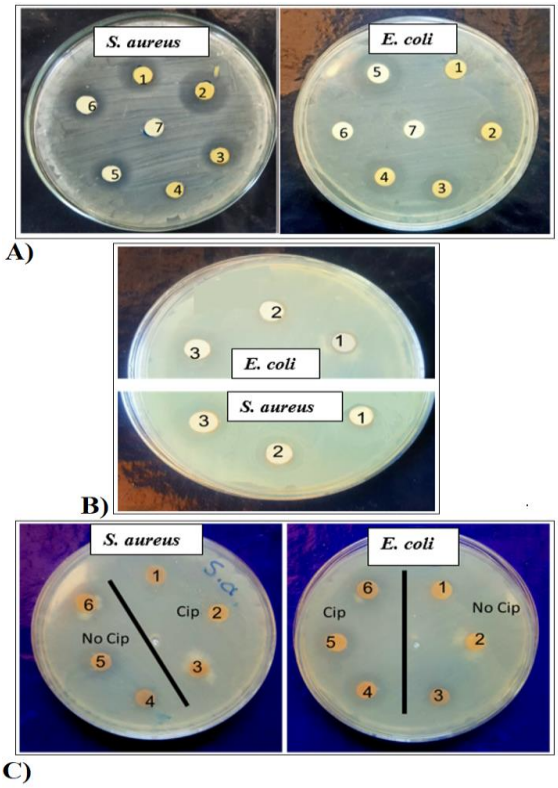

Fig. 9. Antibacterial results and disc diffusion assay on *E.coli* and *S.aureus*: A) Disc diffusion of different samples (1= 300 µg curcumin, 2= 300 µg curcumin with ciprofloxacin, 3= 200 µg curcumin with ciprofloxacin, 4= 100 µg curcumin with

ciprofloxacin, 5= Ciprofloxacin in DMSO, 6= Ciprofloxacin in water, 7= DMSO); B**)** Effects of different nanocomposites (1= G, 2= GC, 3= GCA) on *E.coli* and *S.aureus.* C) Disc diffusion of different nanocomposites (1= G, 2= GC, 3= GCA) carrying curcumin in the presence and absence of ciprofloxacin.

Conclusion

The present study showed that graphene modification by hydrogels like chitosan and sodium alginate would improve its biological characteristics, like protein adsorption and hemolysis, though curcumin loading was not so high. GCA nanocomposite had lower hemolysis and BSA adsorption, which shows its bioavailability and biocompatibility. At last, by comparing the antibacterial results, it can be concluded that curcumin's antibacterial activity is based on species of the bacteria as it did not have any antibacterial effect on *E. coli* and showed an antagonistic effect with ciprofloxacin. But for *S. aureus*, this compound was antibacterial and had a synergistic impact. This property of curcumin should be investigated for more bacteria. Although the GCA nanocomposite did not show any antibacterial effect, results showed that these particles have a good capacity for carrying and loading curcumin for bacterial purposes; they can be used as a safe cargo for curcumin delivery to evaluate its bioavailability and biocompatibility.

Table 2. Zone inhibition of Curcumin solutions (mm).

	DMSO	Cip in dH2O	Cip in DMSO	Cur 100* +Cip	Cur 200 *+Cip	Cur 300* +Cip	Cur 300*
S. aureus	-	13	13	-	17	20	15
E. coli	-	14	10	15	13	12	-
Spot number	7	6	5	4	3	2	1

Cip: Ciprofloxacin; Cur: Curcumin; *= mg/ml

Table 3. Zone inhibition of nanocomposite and curcumin-loaded nanocomposite in the presence of ciprofloxacin (cm).

	G+Cur	GC+Cur	GCA+Cur	G-Cur+Cip	GC-Cur+Cip	GCA-Cur+Cip
S. aureus	0	0	0	12	12	12
E. coli	0	0	0	9	14	13
Spot number	1	2	3	4	5	6

Cip: Ciprofloxacin; Cur: Curcumin

Acknowledgments

The authors express their gratitude to the Research Council of the Shahid Bahonar University of Kerman, Kerman (Iran), for financial support during this project.

Conflict of Interests

The authors declare no conflict of interest.

References

Badoei-Dalfard, A., Tahami, A., & Karami, Z. (2022) Lipase immobilization on glutaraldehyde activated graphene oxide/chitosan/cellulose acetate electrospun nanofibrous membranes and its application on the synthesis of benzyl acetate. *Colloids and Surfaces B: Biointerfaces, 209*, 112151. https://doi.org/10.1016/j.colsurfb.2021.112151.

Bennis, S., Chapey, C., Robert, J., & Couvreur, P. (1994). Enhanced cytotoxicity of doxorubicin encapsulated in polyisohexylcyanoacrylate nanospheres against multidrug-resistant tumour cells in culture. *European Journal of Cancer*, *30*(1), 89-93. https://doi.org/10.1016/S0959-8049(05)80025-5.

Chidambaram, M., & Krishnasamy, K. (2014). Nanoparticulate drug delivery system to overcome the limitations of conventional curcumin in the treatment of various cancers: a review. *Drug Delivery Letters*, *4*(2), 116-127. https://doi.org/10.2174/2210303103999131211110708.

Desai, M. P., Labhasetwar, V., Amidon, G. L., & Levy, R. J. (1996). Gastrointestinal uptake of biodegradable microparticles: effect of particle size. *Pharmaceutical Research*, *13*, 1838-1845. https://doi.org/10.1023/A:1016085108889.

Ghawanmeh, A. A., Ali, G. A., Algarni, H., Sarkar, S. M., & Chong, K. F. (2019). Graphene oxide-based hydrogels as a nanocarrier for anticancer drug delivery.

Nano Research, *12*, 973-990. https://doi.org/10.1007/s12274-019-2300-4.

Goswami, M., Mangoli, S. H., & Jawali, N. (2006). Involvement of reactive oxygen species in the action of ciprofloxacin against *Escherichia coli*. *Antimicrobial Agents and Chemotherapy*, *50*(3), 949-954. https://doi.org/10.1128/AAC.50.3.949-954.2006.

Helson, L. (2013). Curcumin (diferuloylmethane) delivery methods: a review. *Biofactors*, *39*(1), 21-26. https://doi.org/10.1002/biof.1080.

Hu, M., & Mi, B. (2014). Layer-by-layer assembly of graphene oxide membranes via electrostatic interaction. *Journal of Membrane Science*, *469*, 80-87. https://doi.org/10.1016/j.memsci.2014.06.036

Hussain, Z., Thu, H. E., Amjad, M. W., Hussain, F., Ahmed, T. A., & Khan, S. (2017). Exploring recent developments to improve antioxidant, anti-inflammatory and antimicrobial efficacy of curcumin: a review of new trends and future perspectives. *Materials Science and Engineering*: *77*, 1316-1326. https://doi.org/10.1016/j.msec.2017.03.226.

Itzia Azucena, R. C., José Roberto, C. L., Martin, Z. R., Rafael, C. Z., Leonardo, H. H., Gabriela, T. P., & Araceli, C. R. (2019). Drug susceptibility testing and synergistic antibacterial activity of curcumin with antibiotics against enterotoxigenic *Escherichia coli*. *Antibiotics*, *8*(2), 43. https://doi.org/10.3390/antibiotics8020043.

Jalaladdiny, S.S., Badoei-dalfard, A., Karami, Z., & Sargazi, G. (2022) Co-delivery of doxorubicin and curcumin to breast cancer cells by a targeted delivery system based on Ni/Ta core-shell metal-organic framework coated with folic acid-activated chitosan nanoparticles. *Journal of the Iranian Chemical Society*, *19*(10), 4287-4298. https://doi.org/10.1007/s13738-022-02604-w.

Jamil, Q. U. A., Jaerapong, N., Zehl, M., Jarukamjorn, K., & Jäger, W. (2017). Metabolism of curcumin in human breast cancer cells: impact of sulfation on cytotoxicity. *Planta Medica*, *83*, 1028-1034. https://doi.org/10.1055/s-0043-107885.

Kiew, S. F., Kiew, L. V., Lee, H. B., Imae, T., & Chung, L. Y. (2016). Assessing biocompatibility of graphene oxide-based nanocarriers: a review. *Journal of Controlled Release*, *226*, 217-228. https://doi.org/10.1016/j.jconrel.2016.02.015.

Li, L., Zhang, X., Pi, C., Yang, H., Zheng, X., Zhao, L., & Wei, Y. (2020). Review of curcumin physicochemical targeting delivery system. *International Journal of Nanomedicine*, *15*, 9799-9821. https://doi.org/10.2147/IJN.S276201.

Lim, G. P., Chu, T., Yang, F., Beech, W., Frautschy, S. A., & Cole, G. M. (2001). The curry spice curcumin reduces oxidative damage and amyloid pathology in an Alzheimer transgenic mouse. *Journal of Neuroscience*, *21*(21), 8370-8377. https://doi.org/10.1523/JNEUROSCI.21-21-08370.2001.

Ma, Z., Haddadi, A., Molavi, O., Lavasanifar, A., Lai, R., & Samuel, J. (2008). Micelles of poly (ethylene oxide)-b-poly (ε-caprolactone) as vehicles for the solubilization, stabilization, and controlled delivery of curcumin. *Journal of Biomedical Materials Research*, *86*(2), 300-310. https://doi.org/10.1002/jbm.a.31584.

Mehrabi, M., Karami, F., Siah, M., Esmaeili, S., & Khodarahmi, R. (2022). Is curcumin an active suicidal antioxidant only in the aqueous environments? *Journal of the Iranian Chemical Society*, *19*(8), 3441-3450. https://doi.org/10.1007/s13738-022-02538-3.

Mehrabi, M., Esmaeili, S., Ezati, M., Abassi, M., Rasouli, H., Nazari, D., ... & Khodarahmi, R. (2021). Antioxidant and glycohydrolase inhibitory behavior of curcumin-based compounds: synthesis and evaluation of anti-diabetic properties in vitro. *Bioorganic Chemistry*, *110*, 104720. https://doi.org/10.1016/j.bioorg.2021.104720.

Moghaddam, K. M., Iranshahi, M., Yazdi, M. C., & Shahverdi, A. R. (2009). The combination effect of curcumin with different antibiotics against *Staphylococcus aureus*. *International Journal of Green Pharmacy*, *3*(2), 141-143. https://doi.org/10.4103/0973-8258.54906.

Mu, L., & Feng, S. S. (2003). A novel controlled release formulation for the anticancer drug paclitaxel (Taxol®): PLGA nanoparticles containing vitamin E TPGS. *Journal of Controlled Release*, *86*(1), 33-48. https://doi.org/9780429162640.

Mun, S. H., Joung, D. K., Kim, Y. S., Kang, O. H., Kim, S. B., Seo, Y. S., ... & Kwon, D. Y. (2013). Synergistic antibacterial effect of curcumin against methicillin-resistant *Staphylococcus aureus*. *Phytomedicine*, *20*(8-9), 714-718. https://doi.org/10.1016/j.phymed.2013.02.006

Nurunnabi, M., Parvez, K., Nafiujjaman, M., Revuri, V., Khan, H. A., Feng, X., & Lee, Y. K. (2015). Bioapplication of graphene oxide derivatives: drug/gene delivery, imaging, polymeric modification, toxicology, therapeutics and challenges. *RSC Advances*, *5*(52), 42141-42161. https://doi.org/10.1039/c5ra04756k.

Pan, Y., Sahoo, N. G., & Li, L. (2012). The application of graphene oxide in drug delivery. *Expert Opinion on Drug Delivery*, *9*(11), 1365-1376. https://doi.org/10.1517/17425247.2012.729575.

Panyam, J., Williams, D., Dash, A., Leslie-Pelecky, D., & Labhasetwar, V. (2004). Solid-state solubility influences encapsulation and release of hydrophobic drugs from PLGA/PLA nanoparticles. *Journal of Pharmaceutical Sciences*, *93*(7), 1804-1814. https://doi.org/10.1002/jps.20094.

Raja, M. A., Arif, M., Feng, C., Zeenat, S., & Liu, C. G. (2017). Synthesis and evaluation of pH-sensitive, self-assembled chitosan-based nanoparticles as efficient doxorubicin carriers. *Journal of Biomaterials Applications*, *31*(8), 1182-1195. https://doi.org/10.1177/0885328216681184.

Ramazani, A., Abrvash, M., Sadighian, S., Rostamizadeh, K., & Fathi, M. (2018). Preparation and characterization of curcumin loaded gold/graphene oxide nanocomposite for potential breast cancer therapy. *Research on Chemical Intermediates*, *44*, 7891-7904. https://doi.org/10.1007/s11164-018-3593-8.

Richardson, J. J., Cui, J., Bjornmalm, M., Braunger, J. A., Ejima, H., & Caruso, F. (2016). Innovation in layer-by-layer assembly. *Chemical Reviews*, *116*(23), 14828-14867. https://doi.org/10.1021/acs.chemrev.6b00627.

Roudashti, S., Zeighami, H., Mirshahabi, H., Bahari, S., Soltani, A., & Haghi, F. (2017). Synergistic activity of sub-inhibitory concentrations of curcumin with ceftazidime and ciprofloxacin against *Pseudomonas aeruginosa* quorum sensing related genes and virulence traits. *World Journal of Microbiology and Biotechnology*, *33*, 1-8. https://doi.org/10.1007/s11274-016-2195-0.

Sun, X., Liu, Z., Welsher, K., Robinson, J. T., Goodwin, A., Zaric, S., & Dai, H. (2008). Nano-graphene oxide for cellular imaging and drug delivery. *Nano Research*, *1*, 203-212. https://doi.org/10.1007/s12274-008-8021-8.

Surdjawidjaja, J. E. (2012). Antagonism of vitamin C and vitamin E on action of quinolones. *Universa Medicina*, *31*(2), 71-72. https://doi.org/10.18051/UnivMed.2012.v31.71-72.

Teow, S. Y., & Ali, S. A. (2015). Synergistic antibacterial activity of Curcumin with antibiotics against *Staphylococcus aureus*. *Pakistan Journal of Pharmaceutical Sciences*, *28*(6), 2109-2114. https://doi.org/10.21203/rs.3.rs-1551439/v1.

Wang, F., Yuan, J., Zhang, Q., Yang, S., Jiang, S., & Huang, C. (2018). PTX-loaded three-layer PLGA/CS/ALG nanoparticle based on layer-by-layer method for cancer therapy. *Journal of Biomaterials Science*, *29*(13), 1566-1578. https://doi.org/10.1080/09205063.2018.1475941.

Wong, J. K., Mohseni, R., Hamidieh, A. A., MacLaren, R. E., Habib, N., & Seifalian, A. M. (2017). Limitations in clinical translation of nanoparticle-based gene therapy. *Trends in Biotechnology*, *35*(12), 1124-1125. https://doi.org/10.1016/j.tibtech.2017.07.009.

Yadav, A., Lomash, V., Samim, M., & Flora, S. J. (2012). Curcumin encapsulated in chitosan nanoparticles: a novel strategy for the treatment of arsenic toxicity. *Chemico-Biological Interactions*, *199*(1), 49-61. https://doi.org/10.1016/j.cbi.2012.05.011.

Yun, D. G., & Lee, D. G. (2016). Antibacterial activity of curcumin via apoptosis-like response in *Escherichia coli*. *Applied Microbiology and Biotechnology*, *100*, 5505-5514. https://doi.org/10.1007/s00253-016-7415-x.

Zaaba, N. I., Foo, K. L., Hashim, U., Tan, S. J., Liu, W. W., & Voon, C. H. (2017). Synthesis of graphene oxide using modified hummers method: solvent influence. *Procedia Engineering*, *184*, 469-477. https://doi.org/10.1016/j.proeng.2017.04.118.

Zhang, X., Yin, J., Peng, C., Hu, W., Zhu, Z., Li, W., ... & Huang, Q. (2011). Distribution and biocompatibility studies of graphene oxide in mice after intravenous administration. *Carbon*, *49*(3), 986-995. https://doi.org/10.1016/j.carbon.2010.11.005.

Zheng, D., Huang, C., Huang, H., Zhao, Y., Khan, M. R. U., Zhao, H., & Huang, L. (2020). Antibacterial mechanism of curcumin: a review. *Chemistry & Biodiversity*, *17*(8), e2000171. https://doi.org/10.1002/cbdv.202000171.

Zhu, Y., Murali, S., Cai, W., Li, X., Suk, J. W., Potts, J. R., & Ruoff, R. S. (2010). Graphene and graphene oxide: synthesis, properties, and applications. *Advanced Materials*, *22*(35), 3906-3924. https://doi.org/10.1002/adma.201001068.

Zokaei, E., Badoei-Dalfrad, A., Ansari, M., Karami, Z., Eslaminejad, T., & Nematollahi-Mahani, S. N. (2019). Therapeutic potential of DNAzyme loaded on chitosan/cyclodextrin nanoparticle to recovery of chemosensitivity in the MCF-7 cell line. *Applied Biochemistry and Biotechnology*, 1*87*, 708-723. https://doi.org/10.1007/s12010-018-2836-x.